Simulation of Interferometric SAR Response for Characterizing Forest Successional Dynamics

Hongbo Yang, Dawei Liu, Guoqing Sun, Zhifeng Guo, and Zhiyu Zhang

***Abstract*—The dynamics of scattering phase center height (SPCH) in a paper birch stand throughout its succession following clear cutting was studied to improve the interpretation of interferometric synthetic aperture radar (InSAR) response to forest structure changes. A forest growth model (ZELIG) and a fractal tree model (L-system) were utilized together for simulation of the three-dimensional (3-D) structure changes of the stand. Then, a high-fidelity coherent radar scattering model (CORSM) based on 3-D forest structure was employed to simulate the SPCH dynamics of the birch stand. The simulation experiment shows that correlation between L-band SPCH and forest parameters (Lorey's mean height (hL) and biomass) could be noticeably affected by changing pattern of 3-D forest structure at different successional stages, which should be considered in our future exploration of SPCH for forest parameter estimation.**

***Index Terms*—Forest succession, L-system, scattering model, ZELIG.**

I. Introduction

INTERFEROMETRIC synthetic aperture radar (InSAR) is ideal for retrieval of forest structure, since it is particularly sensitive to the 3-D distribution of scattering elements of forest (leaves, branches, and trunks). Fully polarimetric InSAR (POLInSAR) [1], [2] based on the coherent combination of radar interferometry and polarimetry further enhanced the ability for estimating forest structure parameters. If a sufficient number of interferometric baselines are available, tomography can be used to extract vertical forest structure information in much greater detail. Encouraging results have been obtained from previous InSAR polarimetry and tomography studies [3]–[7]. However, it should be recognized that all these aforementioned techniques were tested primarily with airborne InSAR data over selected test sites. For spaceborne SAR missions, such as the ALOS L-band mission and TanDEM-X mission, single-pol and single-baseline InSAR data still seem to be the general means for environmental and forest mapping on a global scale [8], which leads to the necessity of a deep interpretation of single-pol and single-baseline InSAR response to forest structure changes.

Traditional coherent radar models [9]–[11] provide good insight into the expected behavior of radar backscatter from forest canopies, but few studies have dealt with the correlation between forest dynamics after severe disturbances (e.g., clear cutting) and the corresponding InSAR feature changes due to the scarcity of long-term ground truth measurements and InSAR observations on the same ecosystems.

In this letter, a high-fidelity forest radar backscattering simulation system was developed to convincingly simulate the scattering phase center height (SPCH) changes of a paper birch stand throughout its succession, from bare ground to mature forest. This system consists of three models: 1) a parametric L-system [12], which could provide an explicit description of the 3-D distribution of leaves, trunk, and branches of individual birch trees; 2) a forest growth model, ZELIG [13], which could specify the location and height of each tree in the birch stand at different growth phases and will be combined with the L-system to simulate the 3-D structure dynamics throughout the succession of the whole stand; and 3) a 3-D coherent scattering radar model [14], CORSM, which was designed to be based on fractal-generated 3-D structure of vegetation canopies and will be used here for InSAR data, and thus the SPCH simulation. Analysis of the 3-D structure changing pattern of the birch stand, as well as its impacts on the correlation between SPCH and forest structure parameters (Lorey's mean height (hL) and biomass) throughout the successional process, is presented in this letter.

II. Model Description and Simulations

In this letter, we simulated the forest succession following clear cutting of a 60 m $\times$ 80 m paper birch stand in the Northern Experimental Forest (NEF) located in Howland, ME $(45°15'\text{N}, 68°45'\text{W})$, where paper birch is one of the dominant species. The proposed 3-D forest structure and corresponding SPCH dynamics simulation comprise four major steps, as follows:

1) Based on field measurements of birch tree geometrical features, construct the 3-D architecture of individual birch trees with different heights using parametric L-system and form an individual tree 3-D structure library;
2) Simulate the birch stand succession following clear cutting and output the distribution information of all individual trees within the birch stand at different growth phases using ZELIG model;

Manuscript received November 21, 2012; revised April 7, 2013, June 29, 2013, September 27, 2013, November 6, 2013, and December 30, 2013; accepted December 31, 2013. This work was supported in part by the National Basic Research Program of China under Grant 2013CB733401, by the Special Foundation for Young Scientists of the State Laboratory of Remote Sensing Sciences (RC12), by the Strategic Priority Research Program—"Climate Change: Carbon Budget and Related Issues" of the Chinese Academy of Sciences under Research Grant XDA05050100, and by the National Natural Science Foundation of China under Research Grants 41171283 and 41105007.

H. Yang, Z. Guo, and Z. Zhang are with the State Key Laboratory of Remote Sensing Science, Institute of Remote Sensing and Digital Earth, Chinese Academy of Sciences, Beijing 100101, China.

D. Liu is with the School of Electronic and Information Engineering, BeiHang University, Beijing 100191, China (e-mail: dawliu@gmail.com).

G. Sun is with the Department of Geography and the Earth System Science Interdisciplinary Center, University of Maryland, College Park, MD 20742 USA.

Color versions of one or more of the figures in this paper are available online at http://ieeexplore.ieee.org.

Digital Object Identifier 10.1109/LGRS.2014.2298431

TABLE I
DESCRIPTION OF INDIVIDUAL PAPER BIRCH TREE

Height of tree		2~6m	7~16m	17~25m
Leaf	Radius(cm)	3.5	3.5	3.5
	Thickness(mm)	0.15	0.15	0.15
	Density(K/m^3)	490~450	420~400	480~350
Branch	Density(N/m^3)	80~50	45~30	25~20
Trunk	DBH (cm)	3.0~5.4	6.2~19.6	21.4~38.6
Crown	Height(m)	1.1~3.5	3.9~9.2	9.4~14.3
	Width(m)	0.6~1.5	1.8~4.7	5.0~7.8

3) Construct 3-D birch stand structure at each growth phase using tree distribution information provided by ZELIG and the 3-D structure of each tree already prepared by L-system;
4) With these 3-D forest stands at different growth phases as input, simulate the corresponding InSAR image pairs using CORSM and retrieve the SPCHs.

A. Modeling the 3-D Structure of Individual Trees

L-system, an effective tool to simulate geometrical features of tree-like structure, has been successfully used in previous electromagnetic scattering modeling studies to examine the coherent [9] or multiple scattering [15] effect. In this letter, a parametric L-system was employed to generate the 3-D structure of individual birch trees of different heights, and thus form a 3-D structure library for birch stand simulation. Field measurements of basic structural parameters (e.g., the DBH, height, leaf density, leaf thickness, branch density, branch angle, and crown size) and the relationship between the length and diameter of new branches and those of their originating branches were used to properly take into account the botanical properties of paper birch for the 3-D model construction. Major structural parameters of individual paper birch trees are listed in Table I.

We constructed a 3-D structure library of paper birch with individual tree heights ranging from 1 m to 25 m, at 0.5 m intervals, to represent all possible birch trees that may occur in the birch stand throughout the successional process.

B. Simulation of Forest Succession

ZELIG is a gap model that has been successfully validated and applied in previous forest succession modeling studies [16], [17]. It was selected for this study because it is an individual tree-based model, which could simulate the birth, growth, and death of every individual tree within the stand in response to environmental constraints (e.g., temperature, light, and precipitation) and provide its biophysical parameters. To simulate the succession of birch forest after clear cutting, ZELIG requires botanical and living environmental information as input. The botanical information includes the species' maximum age, DBH and height $(\mathrm{Age}_{\max}, \mathrm{DBH}_{\max}, \mathrm{Height}_{\max})$, growth rate parameter (G), minimum and maximum growing degree-days limits $(\mathrm{DD}_{\min}, \mathrm{DD}_{\max})$, and tolerance class for shade, nutrient stress, and drought (TS, TN, TD). For paper birch, these parameters can be found in the files on a ZELIG website [18] and are listed in Table II. While the environmental data chosen, including the monthly precipitation and temperature, was the average monthly data over the past decade (2000 to 2010) of the NEF and could be obtained from a weather history website [19]. The biophysical information for individual trees within the stand provided by ZELIG includes DBH, height, above ground woody biomass (biomass), etc. Some extensions have been applied to the ZELIG model in order for it to properly work with the L-system for 3-D forest architecture construction. For instance, to get the specific location of each tree, ZELIG was modified in this study to assign random coordination for every tree as it is generated and the coordination will be fixed in the following stages until the tree is dead and disappears from the stand.

TABLE II
BOTANICAL PARAMETERS OF BIRCH

$\mathrm{Age}_{\max}$ (year)	140	$\mathrm{DD}_{\max}$	2500
$\mathrm{DBH}_{\max}$ (cm)	100	TS	4
$\mathrm{Height}_{\max}$ (m)	25	TN	3
G	160	TD	3
$\mathrm{DD}_{\min}$	700		

We modeled the successional process of a 60 m $\times$ 80 m paper birch stand from bare ground to mature forest. To ensure this was long enough to observe the correlation between SPCH and forest parameters at different succession stages, we chose 300 years as the time span for this simulation. Simulation results were recorded at 5-year intervals. hL was calculated for each birch stand to characterize the forest structure dynamics with following equation:

$$\mathrm{h}L = \sum_{i=1}^{N} \frac{A_i}{\left(\sum_{j=1}^{N} A_j\right)} H_i \tag{1}$$

where H_i and A_i are the height and basal area of each individual tree within the birch stand, respectively. N is the total number of trees within the stand.

C. Construction of 3-D Forest Structure

With the coordination and height information of each tree in the birch stand at different growth phases provided by ZELIG and the height-specific 3-D architecture of individual trees in the birch tree structure library generated by the L-system, we were able to generate the 3-D structure of all 60 birch stands for InSAR data simulation. Fig. 1 shows a sample 10 m $\times$ 10 m plot in the paper birch stand at two different growth phases (10 and 50 years, respectively).

D. Retrieval of SPCH From Simulated InSAR Data

CORSM is a coherent radar backscattering model based on fractal-generated 3-D forest scenarios. Compared with other radar models [9]–[11], it can more properly consider the impacts of forest heterogeneity on radar backscattering. With the 3-D structure of the 60 birch stands as input, complex radar image pairs were generated using CORSM. JPL TOPSAR configuration (platform height 8500 m, baseline length 2.6 m, baseline angle 62.77°, incidence angle 35°) was adopted in the

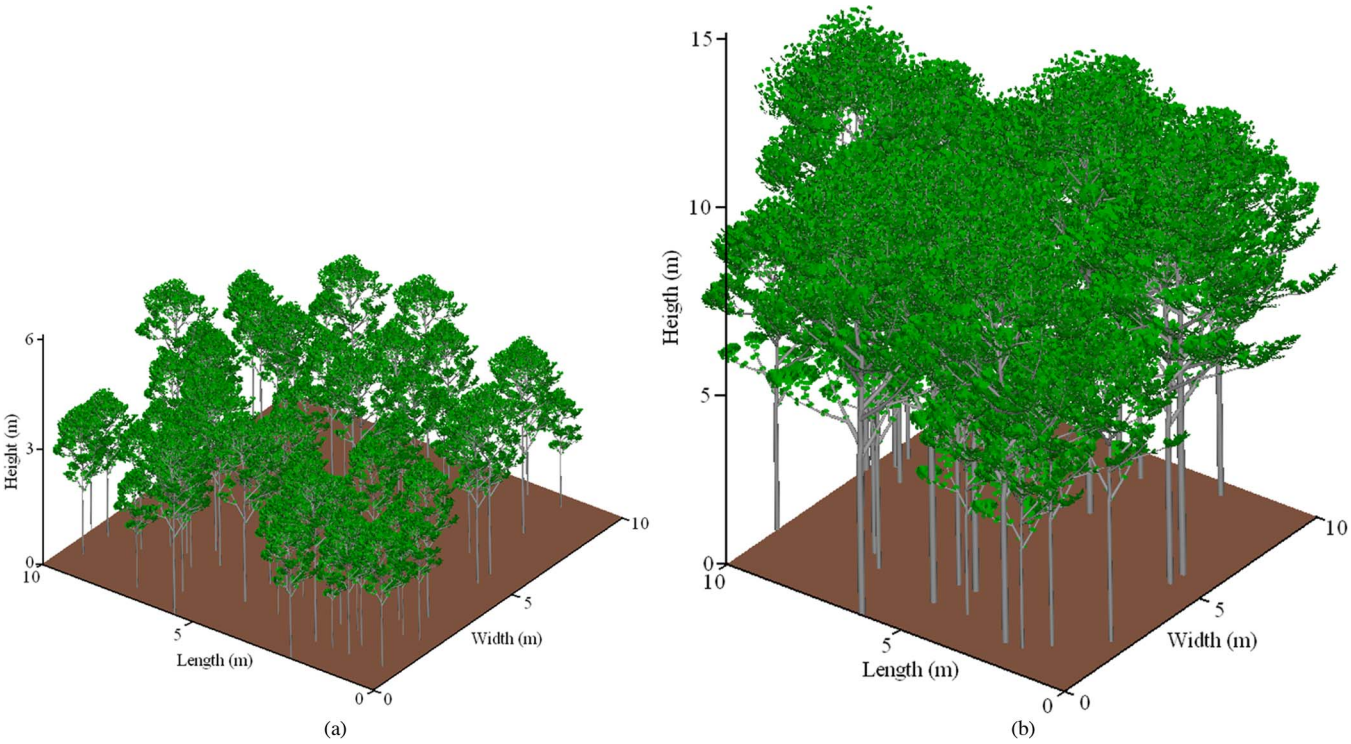

Fig. 1. Automatically generated 3-D structure of a 10 m × 10 m sample plot within a birch forest stand located in Howland, ME, at different growth phases through combined use of ZELIG model and L-system: (a) the 3-D structure of the birch stand at 10 years; (b) the 3-D structure of the birch stand at 50 years.

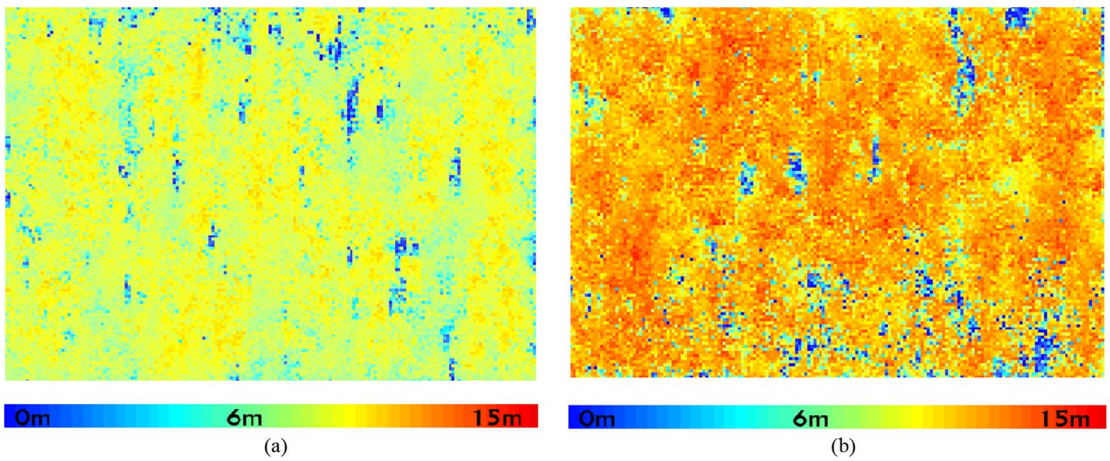

Fig. 2. SPCH derived from simulated InSAR L band VV images of the birch forest stand located in Howland, Main, at different growth phases. (a) SPCH of the birch stand at age of 50 with an hL of 12.3 m; (b) SPCH of the birch stand at age of 100 with an hL of 18.7 m.

InSAR data simulation process. Once InSAR image pairs were created, SPCH was estimated using the following equation:

$$\mathrm{SPCH} = \frac{(\Delta\varphi' - \Delta\varphi) \cdot \lambda \cdot r \cdot \sin\theta}{2\pi \cdot B_{\perp}} \tag{2}$$

where H is the platform height; r is the range distance; α is the baseline angle; $B_{\perp}$ is the perpendicular baseline length; λ is the wavelength; $\Delta\varphi = \angle(E_1^* \cdot E_2)$ represents the phase difference between the signal E_1 and E_2 received by the two antennas (i.e., the difference between the phase of pixel in the master image and the phase of its counterpart in the slave image); $\Delta\varphi'$ represents the phase difference of the signal reflected by the bare ground surface within the same range distance.

For illustration purposes, high-resolution SPCH images (pixel size is 0.5 m) of the birch stand at 50 and 100 years were simulated and presented in Fig. 2. Notably, as the forest ages from 50 to 100 (hL increases from 12.4 m to 18.7 m), SPCH increases noticeably as well. This holds true for most cases, higher forest height usually results in higher SPCH.

III. Results and Discussion

A. Sensitivity Analysis of SPCH to Forest Successional Dynamics

With CORSM, L-band co-polarized (HH and VV) complex radar image pairs of all 60 3-D birch stands at different growth

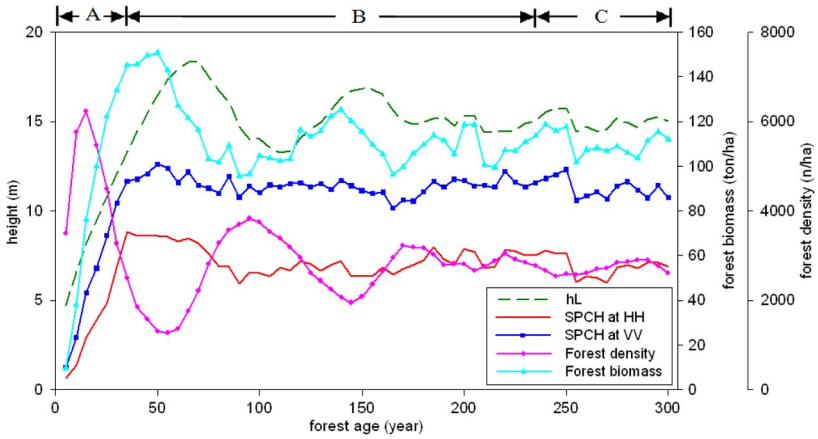

Fig. 3. Birch forest parameters (hL, density, and biomass) and L-band SPCH (at both HH and VV polarizations) dynamics as the birch stand regrows from bare ground.

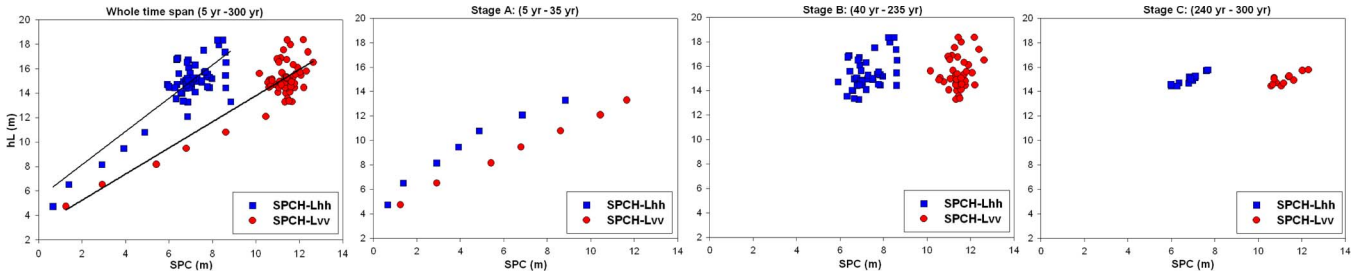

Fig. 4. L-band SPCH at HH (blue squares) and VV (red circles) polarizations versus hL over the whole time span and the three different stages.

phases were generated for SPCH estimation. The pixel size was set as 10 m; the average SPCH of the 48 pixels within the 60 m $\times$ 80 m birch stand represents the SPCH of the birch stand as a whole. Simulation results are presented in Fig. 3, in which forest density, biomass, and hL of each birch stand were derived from the individual birch tree information provided by ZELIG. For clarity, the 300 year time span was divided into three succession stages: 1) stage A: early fast growing stage, ranging from 5 to 35 years; 2) stage B: transitional stage, ranging from 40 to 230 years; 3) stage C: mature stage, ranging from 235 to 300 years.

During stage A, the young forest grows very fast. The forest canopy structure is relatively simple and homogeneous because most of the individual trees have similar ages, and thus, similar structure. Although the forest density decreases rapidly after an age of approximately 20 years, only a small canopy gap will be produced due to the remaining relatively high density and small tree structure. SPCH reflected this change well. A linear relationship was observed among SPCH (both at HH and VV polarizations), biomass, and hL during this stage.

During stage B, however, the SPCH seems to be "saturated" and becomes stable, regardless of how noticeably the hL and biomass change. As shown in Fig. 3, for both the hL and biomass, there are two significant peaks (around ages of 60 and 150) within this stage, but the SPCH only vibrates within a small range. Nevertheless, this is not because the sensitivity of SPCH to the forest structure dynamics decreases as the forest ages, but because the effect of hL vibrations on SPCH was largely counteracted by the effect of forest density changes. Take the first peak of hL that happens around 60 years as an example; after a short period of rapid growth in forest density between the ages of 5 and 20, many small trees living under or near tall trees begin to die due to increasingly fierce competition for limited environmental resources. As a result, the forest density decreased rapidly, while the hL kept growing between the ages of 20 and 70. Subsequently, some large trees also die due to the ongoing competition. Noticeable intertree gaps are thus formed and a greater number of small trees occupy these spaces to grow. Therefore, the density was restored to some extent; meanwhile, the hL decreased for trees between the ages of 70 and 90. This process repeats during between the ages of 110 and 170, on a smaller scale. A previous study [20] has shown that, with the same height, lower forest density results in lower SPCH because the direct scattering from the ground and the ground bounce contributions are stronger. Therefore, within stage B, the impact of hL changes on the SPCH was largely counteracted by the effect of forest density changes, so the SPCH remains relatively stable.

During stage C, the forest reaches maturity, and the forest density becomes stable. The SPCH vibrates within a small range and is generally in tune with biomass and hL vibrations.

B. Correlations Among SPCH, HL, and Biomass

In this letter, we further investigated the correlation between SPCH and two important forest biophysical parameters, hL and biomass, throughout the successional process.

Fig. 4 shows the correlation between the hL and the L-band SPCH over the entire time span and the three different succession stages, respectively. The general linear regression relation is

$$\begin{aligned} \mathrm{hL} &= 5.439 + 1.359 \cdot \mathrm{SPCH}_{HH}, \mathrm{R}^2 = 0684 \\ \mathrm{hL} &= 3.109 + 1.069 \cdot \mathrm{SPCH}_{VV}, \mathrm{R}^2 = 0.752. \end{aligned} \quad (3)$$

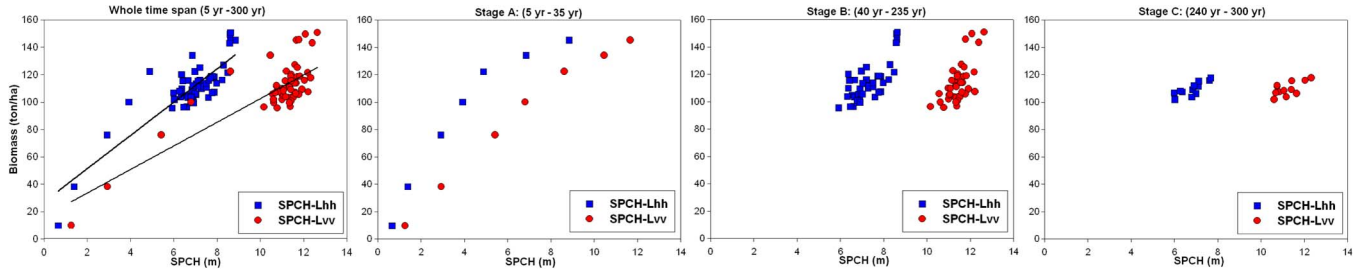

Fig. 5. L-band SPCH at HH (blue squares) and VV (red circles) polarizations versus biomass over the whole time span and the three different stages.

Fig. 5 shows the corresponding correlation between the forest biomass and SPCH. The general linear regression relation is

$$Biomass = 27.079 + 12.157 \cdot \mathrm{SPCH}_{HH}, \mathrm{R}^2 = 0.729$$
$$Biomass = 16.315 + 8.629 \cdot \mathrm{SPCH}_{VV}, \mathrm{R}^2 = 0.653. \quad (4)$$

Generally, both hL and biomass have a good correlation with SPCH at either stage A or stage C, when the forest structure is relatively uniform. However, during stage B, the hL changes drastically, but the effect of the hL vibrations on SPCH was largely counteracted by changes in the forest density. It is obvious that the relationship between hL and SPCH is not a good linear relationship. Compared with hL, there is a better relationship between SPCH and biomass during stage B. This may be due to the penetration ability of the microwave into the forest canopy. Therefore, SPCH remains sensitive to the stem volume, and thus, the biomass changes.

IV. Conclusion

In this letter, we simulated forest dynamics following clear cutting of a paper birch stand and the corresponding SPCH changes through combined use of ZELIG, L-system, and CORSM. The simulation results showed that the correlation between the SPCH and the hL, or biomass, is not always a positive correlation at different succession stages. Generally, during the early fast growing stage and the mature stage (stage A and stage C), SPCH could serve as a good indicator for forest dynamics. During the transitional stage (stage B) between them, however, the relationship between SPCH and hL, or biomass, is not so good. The effect of hL fluctuation on the SPCH, in particular, is largely counteracted by changes in forest density. Therefore, complex forest age composition might pose an additional challenge in exploration of L-band InSAR data, such as InSAR data from PALSAR and the planned PALSAR-2 (launch 2013) missions, for large-scale forest parameter retrieval using SPCH.

Note that neither InSAR decorrelation nor multiscattering among scatters was taken into account in this simulation process. The relationship found in this study will not be exactly as shown in real cases. However, understanding of the effect will still be useful and provide insight on what information the InSAR data can provide. Further investigation will clarify whether the correlation changing pattern is consistent with real cases, using field measurements and observed InSAR data.

Acknowledgment

The authors would like to thank the editor and reviewers of this letter for their insightful remarks that have helped improve this manuscript.

References

[1] S. R. Cloude and K. P. Papathanassiou, "Polarimetric SAR interferometry," *IEEE Trans. Geosci. Remote Sens.*, vol. 36, no. 5, pp. 1551–1565, Sep. 1998.
[2] K. P. Papathanassiou and S. R. Cloude, "Single-baseline polarimetric SAR interferometry," *IEEE Trans. Geosci. Remote Sens.*, vol. 39, no. 11, pp. 2352–2363, Nov. 2001.
[3] M. Neumann, S. S. Saatchi, L. M. H. Ulander, and J. E. S. Fransson, "Assessing performance of L- and P-band polarimetric interferometric SAR data in estimating boreal forest above-ground biomass," *IEEE Trans. Geosci. Remote Sens.*, vol. 50, no. 3, pp. 714–726, Mar. 2012.
[4] Hajnsek, F. Kugler, S. K. Lee, and K. P. Papathanassiou, "Tropical-forest-parameter estimation by means of Pol-InSAR: The INDREX-II campaign," *IEEE Trans. Geosci. Remote Sens.*, vol. 47, no. 2, pp. 481–493, Feb. 2009.
[5] M. M. d'Alessandro and S. Tebaldini, "Phenomenology of P-band scattering from a tropical forest through three-dimensional SAR tomography," *IEEE Geosci. Remote Sens. Lett.*, vol. 9, no. 3, pp. 442–446, May 2012.
[6] E. Aguilera, M. Nannini, and A. Reigber, "A data-adaptive compressed sensing approach to polarimetric SAR tomography of forested areas," *IEEE Geosci. Remote Sens. Lett.*, vol. 10, no. 3, pp. 543–547, May 2013.
[7] Frey and E. Meier, "Analyzing tomographic SAR data of a forest with respect to frequency, polarization, and focusing technique," *IEEE Trans. Geosci. Remote Sens.*, vol. 49, no. 10, pp. 3648–3659, Oct. 2011.
[8] Praks, O. Antropov, and M. T. Hallikainen, "LIDAR-aided SAR interferometry studies in boreal forest: scattering phase center and extinction coefficient at X- and L-band," *IEEE Trans. Geosci. Remote Sens.*, vol. 50, no. 10, pp. 3831–3843, Oct. 2012.
[9] Y. C. Lin and K. Sarabandi, "A Monte Carlo coherent scattering model for forest canopies using fractal-generated trees," *IEEE Trans. Geosci. Remote Sens.*, vol. 37, no. 1, pp. 440–451, Jan. 1999.
[10] Sarabandi and Y. C. Lin, "Simulation of interferometric SAR response for characterizing thescattering phase center statistics of forest canopies," *IEEE Trans. Geosci. Remote Sens.*, vol. 38, no. 1, pp. 115–125, Jan. 2000.
[11] Thirion, E. Colin, and C. Dahon, "Capabilities of a forest coherent scattering model applied to radiometry, interferometry, and polarimetry at P-and L-band," *IEEE Trans. Geosci. Remote Sens.*, vol. 44, no. 4, pp. 849–862, Apr. 2006.
[12] P. Prusinkiewicz and A. Lindenmayer, *The Algorithmic Beauty of Plants*. New York, NY, USA: Springer-Verlag, 1990.
[13] D. L. Urban, *A Versatile Model to Simulate Forest Pattern: A User's Guide to ZELIG Version 1.0*. Charlottesville, VA, USA: Univ. of Virginia Press, 1990.
[14] D. W. Liu, G. Q. Sun, Z. F. Guo, K. J. Ranson, and Y. Du, "Three-dimensional coherent radar backscatter model and simulations of scattering phase center of forest canopies," *IEEE Trans. Geosci. Remote Sens.*, vol. 48, no. 1, pp. 349–357, Jan. 2010.
[15] G. F. Zhang, L. Tsang, and Z. X. Chen, "Collective scattering effects of trees generated by stochastic Lindenmayer systems," *Microw. Opt. Technol. Lett.*, vol. 11, no. 2, pp. 107–111, Feb. 1996.
[16] G. R. Larocque, L. Archambault, and C. Delisle, "Modelling forest succession in two southeastern Canadian mixedwood ecosystem types using the ZELIG model," *Ecol. Model.*, vol. 199, no. 3, pp. 350–362, Dec. 2006.
[17] S. W. Seagle and S. Y. Liang, "Application of a forest gap model for prediction of browsing effects on riparian forest succession," *Ecol. Model.*, vol. 144, no. 2/3, pp. 213–229, Oct. 2001.
[18] [Online]. Available: http://www.eco.wiz.uni-kassel.de/model_db/mdb/zelig.html
[19] [Online]. Available: http://weather.org/weatherorg_records_and_averages.htm
[20] H. Yang, G. Sun, Z. Guo, and D. Liu, "Simulations of scattering phase center of three-dimensional forest stands generated by lindenmayer system," *Remote Sens. Inf.*, vol. 28, pp. 56–61, Apr. 2013.